

Cite this: *Soft Matter*, 2012, **8**, 10472

www.rsc.org/softmatter

PAPER

## A surfactant-assisted unimolecular platform for multicolor emissions†

Li Zhao, Xinhao Cheng, Yi Ding, Yun Yan\* and Jianbin Huang\*

Received 20th July 2012, Accepted 9th August 2012

DOI: 10.1039/c2sm26678d

We present here a simple molecular assembly approach to multicolor emissions based on a unimolecular platform of a terthiophene-containing amphiphile TTC4L. The amphiphiles self-assemble into vesicles in solution which exhibit a blue emission. Upon controlling the distance between the fluorescent terthiophene groups by transformation of the self-assembly of TTC4L molecules into their co-assembly with surfactants, the color of the emissions can be continuously tailored which covers most of the visible region. Since the multi-colors were obtained without any structural modification on the fluorescent molecules, we have demonstrated a real unimolecular platform for fabricating multicolor emissions. In contrast, only dual emissions can be obtained from TTC4L using host–guest chemistry. As a simple approach of ‘tunable emissions’, this surfactant-assisted unimolecular platform opens a new vista for the application of molecular assemblies in advanced light emitting materials.

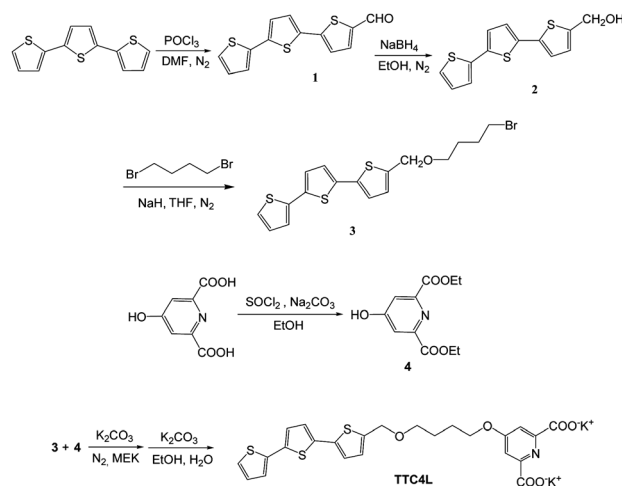
## Introduction

Multicolor emissions have been the subject of intense academic research because of their potential applications in full color displays and white lightening devices.<sup>1–4</sup> So far, this has been achieved by molecular engineering endeavors *via* attachment of various substituent groups to the central fluorescent groups.<sup>5–11</sup> However, this chemical approach has limitations in terms of laborious, multistep processes, and a lack of generality for a single synthesis.<sup>12</sup> Therefore, it is highly desired to create versatile fluorescent emissions from exactly the same molecule which should not suffer any chemical modifications. To this end, host–guest chemistry was employed to obtain tunable emissions.<sup>13–20</sup> It has been found that many fluorescent groups may exhibit distinct emissions before and after host–guest complexation, which provides a protocol to achieve dual fluorescence,<sup>13,18</sup> yet it remains a challenge to obtain multiple colors from this strategy.

Considering the analogies of host–guest chemistry and molecular self-assembly, we are inspired to tune the fluorescence of the ‘guest’ molecules with the assistance of amphiphiles. To make multicolor emissions based on a unimolecular platform a reality, we designed a terthiophene amphiphile TTC4L as illustrated in Scheme 1. The choice of terthiophene as the fluorescent

group lies in its interesting optical and electronic properties that have been verified applicable in many fields.<sup>7,21–25</sup> Moreover, the oligothiophenes exhibit unique versatile emissions depending on the intermolecular distance.<sup>26–28</sup> If the distance between the terthiophene groups is around 3–4 Å,  $\pi$ – $\pi$  stacking may occur which allows a blue emission;<sup>27,29</sup> when the distance is increased to 4–7 Å, one may obtain green emissions from the excimers.<sup>26,30</sup> At distances larger than 7 Å, there will be no interaction between the terthiophene groups so that one obtains a violet emission from the monomers.<sup>6,30,31</sup>

However, so far, the intermolecular distance dependant fluorescent behavior of oligothiophenes hasn’t been sufficiently exploited to produce multiple emissions. This is partly limited by the poor solubility of oligothiophene derivatives due to the



Scheme 1 Synthesis of TTC4L.

Beijing National Laboratory for Molecular Sciences (BNLMS), State Key Laboratory for Structural Chemistry of Unstable and Stable Species, College of Chemistry and Molecular Engineering, Peking University, Beijing, 100871, P. R. China. E-mail: yunyan@pku.edu.cn; jbhuan@pku.edu.cn

† Electronic supplementary information (ESI) available: the synthesis of TTC4L; species distributions and turbidity curve of TTC4L; fluorescence lifetime of TTC4L and TTC4L–DEAB systems; normalized emission spectra of TTC4L–DEAB system; emission spectra and photographs of TTC4L–C<sub>12</sub>C<sub>4</sub>C<sub>12</sub>, TDPS, C<sub>14</sub>DMAO, TX100 and SDS systems; <sup>1</sup>H NMR spectra of TTC4L– $\beta$ CD systems; fluorescence spectra of TTC4L– $\beta$ CD systems. See DOI: 10.1039/c2sm26678d

strong aggregation tendency driven by  $\pi$ - $\pi$  stacking.<sup>6,32–34</sup> To overcome this problem, a pH sensitive bulky ionic head group was introduced to TTC4L, as demonstrated in Scheme 1. This design allows for the desired solubility as well as the ability of TTC4L to self-assemble at a suitable pH. Upon introduction of amphiphiles to the TTC4L aqueous system, we expect that the self-assembly of TTC4L may be replaced by the co-assembly formed by TTC4L and the added amphiphiles. At suitable amphiphilic concentrations, there would be oligothiophenes of various distances, so that multicolors can be obtained simply by variation of the concentration of surfactants. Herein we show that the addition of simple amphiphiles such as surfactants indeed allows for tunable multicolor emissions which may cover most of the visible range.

## Experimental

### Materials

TTC4L was designed and synthesized in our lab as demonstrated in Scheme 1. Details for this synthesis and characterization are given in the ESI†. Tetradecyl dimethylammonium propane sulfonate (TDPS, Sigma-Aldrich) and sodium dodecyl sulfate (SDS, Acros) were used as received. Dodecyltriethyl ammonium bromide (DEAB) and cetyl trimethyl ammonium bromide (CTAB) were prepared by reactions of 1-bromododecane with corresponding amines, followed by recrystallizing five times from ethanol–acetone. The Gemini surfactant alkanediyl-1,12-bis-(dodecyltriethylammonium bromide) ( $[\text{C}_{12}\text{H}_{25}(\text{CH}_3\text{CH}_2)_2\text{-N}(\text{CH}_2)_4\text{N}(\text{CH}_2\text{CH}_3)_2\text{C}_{12}\text{H}_{25}]\text{Br}_2$ , abbreviated as  $\text{C}_{12}\text{C}_4\text{C}_{12}(\text{Et})$ ) was synthesized according to the procedure reported.<sup>35</sup> Tetradecyl dimethyl amine oxide ( $\text{C}_{14}\text{DMAO}$ , Clariant) was prepared by freeze drying 70% aqueous solution, followed by recrystallizing more than two times from acetone. The purities of the surfactants were examined by the lack of minima in their surface tension curves. The water used was re-distilled from potassium permanganate. The other reagents were of analytical reagent grade.

### Sample preparation

The solutions were obtained by dissolving the solid TTC4L powder in ultrapure water (Milli-Q, 18.2 M $\Omega$  cm). The pH of TTC4L solutions was adjusted to about 9.0 by adding a small enough amount of concentrated KOH aqueous solution to ignore the volume change. Corresponding solutions were prepared by mixing TTC4L solution and concentrated surfactant aqueous solutions of negligible quantity in ultrapure water. These samples were vortex mixed and kept at 25 °C. The pH values were measured using a SevenMulti type pH meter with InLab Semi-Micro electrodes (Mettler Toledo, Switzerland). All analytical measurements were performed at 25 °C.

### Dynamic light scattering (DLS) measurements

DLS measurements were performed with an ALV/DLS/SLS-5022F light scattering-apparatus, equipped with a 22 mW He–Ne laser operating at a wavelength of 632.8 nm with a refractive index matching bath of filtered toluene surrounding the

cylindrical scattering cell. The samples were filtered through 450 nm filters. The scattering angle was 90°.

### TEM observation

A JEOL-100 CX II transmission electron microscope (TEM) was employed to observe the morphology of the vesicles. Drops of samples were put onto 230 mesh copper grids coated with Formvar film. Excess water was removed followed by staining the film negatively with uranyl acetate. After removal of the excess staining liquid by filter paper, samples were then allowed to dry in ambient air at room temperature, before TEM observation.

### Spectroscopic measurements

A Hitachi F-4500 fluorescence spectrometer was used to measure the fluorescence emission of TTC4L–surfactant solutions. The time-resolved fluorescence spectrum measurement was performed with a Lifespec Red spectrofluorometer of Edinburgh Instruments equipped with a Hamamatsu picosecond light pulser C8898 using a 372 nm laser with a repetition rate of 1 MHz as the light source. For each measurement, at least 3000 photon counts were collected in the peak channel to ensure the decay quality. The quality of fit for the decay curves was supported by the fact that the fitting parameter  $\chi^2$  was less than 1.3. UV-vis spectra for all the samples were recorded on a HITACHI spectrophotometer in the visible range of 200–800 nm. The scan rate for each measurement was 10 nm min<sup>−1</sup>.

## Results and discussion

### Properties of TTC4L aqueous system

The synthesis of TTC4L was illustrated in Scheme 1. <sup>1</sup>H NMR and elemental analysis verified the success of this synthesis (Details of the synthesis and characterization of structure of TTC4L can be found in the ESI†). TTC4L is soluble in water at concentrations below 1 mM at pH > 8, and a strong Tyndall effect, which is caused by the scattering of colloidal particles, may be observed at concentrations down to 0.01 mM in the pH range of 8–12, demonstrating the strong self-assembling ability of TTC4L. For the convenience of measurements, a solution of pH 9.0 was chosen for further analysis (See Fig. S1† for the component distribution in TTC4L solutions at various pH).

DLS measurements indicated the presence of particles with average hydrodynamic radii of about 100 nm, which didn't show obvious concentration dependence (Fig. 1a). TEM observations verified that these particles are vesicles (Fig. 1b). The diameters of the vesicles are in the range of 100–300 nm, which is in good agreement with the DLS measurements.

The vesicular suspension of TTC4L exhibits intense blue fluorescence which red shifts with increasing concentration. It can be seen from Fig. 2a that upon increasing the concentration from 0.01 to 1 mM, the fluorescence emission increases from 456 to 475 nm. The red-shift of the fluorescence indicates parallel packing of the terthiophene groups in the form of H-aggregates.<sup>32,36</sup> Such a conclusion was confirmed further by the occurrence of a blue shift in the UV spectra.<sup>33,37–40</sup> It is shown in Fig. 2b that the  $\pi$ - $\pi^*$  transition band occurs at 343 nm for the aqueous TTC4L vesicular suspensions but at 360 nm in ethanol

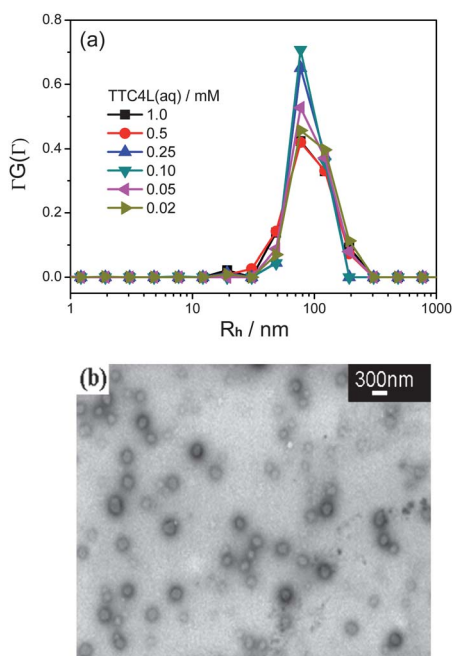


**Fig. 1** (a) DLS results of TTC4L aqueous solution at various concentrations. (b) TEM image of 1 mM TTC4L aqueous solutions at pH 9.0.

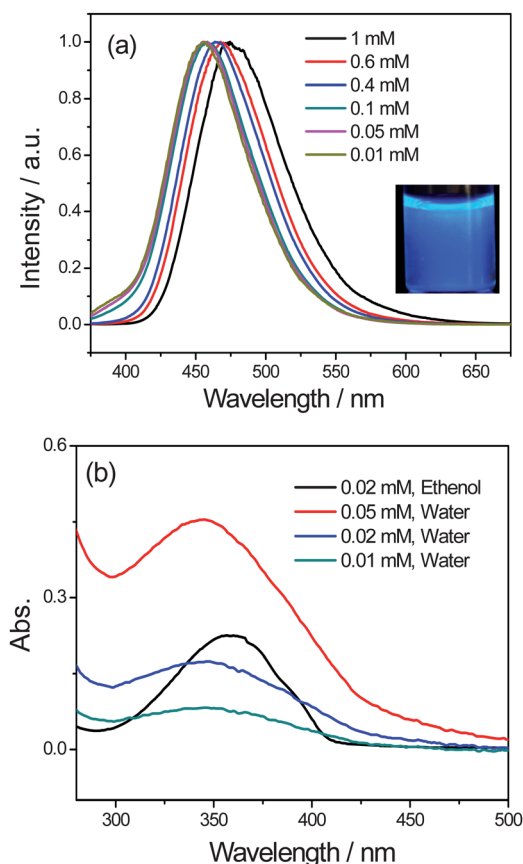


**Fig. 2** Emission (a) and absorption (b) spectra of TTC4L aqueous solutions at various concentrations. The inset in (a) is an image of 0.1 mM TTC4L solution under 365 nm UV light.

where TTC4L forms a molecular solution.<sup>27,41</sup> The occurrence of H-aggregates suggests that the terthiophene groups are  $\pi$ -stacked,<sup>33</sup> which allows for a characteristic blue emission, as demonstrated in Fig. 2a.

### Tuning fluorescence emission by forming co-assembly

The emissions of TTC4L can be changed upon the addition of oppositely charged amphiphiles to break the self-assembly.<sup>42–44</sup> As demonstrated in Fig. 3a (and Fig. S2†), upon addition of 12 mM cationic surfactant DEAB (terethylammonium bromide) to 0.1 mM TTC4L, the peak of the spectrum shifts from 455 (Fig. 3a, curve 1) to 506 nm (Fig. 3a, curve 2), corresponding to an emission change from blue to green (Inset in Fig. 3a). At 12 mM DEAB, the emission spectrum is rather broad and structureless, which is the characteristic emission from excimers.<sup>45,46</sup> This broad feature of the spectrum occurs in wide DEAB concentrations of 5–18 mM. Upon further increasing the concentration of DEAB to over 20 mM, the spectrum blue-shifts again, and the emission of monomeric terthiophene occurs at 439 nm with a shoulder peak at around 420 nm (Fig. 3a, curve 3).<sup>31,47</sup>

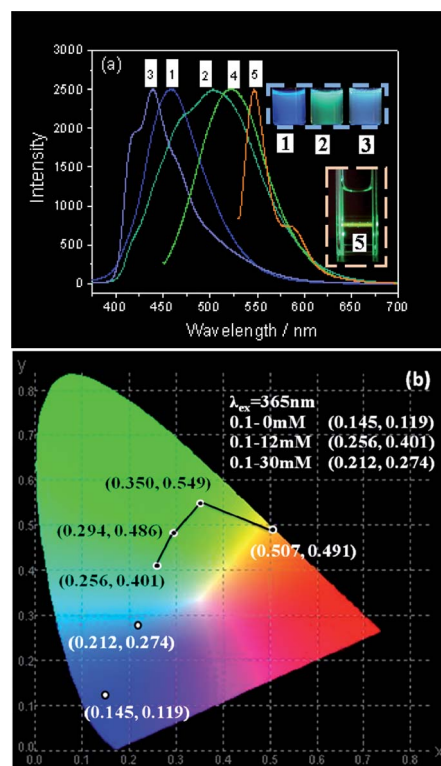


**Fig. 3** (a) Normalized emission spectra of 0.1 mM TTC4L aqueous solution excited at 360 nm in the presence of 0 (curve 1), 12 (curve 2), and 30 (curve 3) mM DEAB, respectively. Curves 4 and 5 are the normalized emission spectra for the 12 mM DEAB system excited at 440 and 520 nm, respectively. The inset images 1, 2, and 3 demonstrate the color of the emissions under 365 nm UV light induced by 0, 12, and 30 mM DEAB, respectively. Image 5 shows the yellow beam pass in the 12 mM DEAB system when irradiated with 532 nm laser. (b) Emission color of 0.1 mM TTC4L solutions in a CIE 1931 chromaticity diagram (The dots connected by the black line show the location of 0.1–12 mM solution irradiated at 365, 400, 440, and 520 nm, respectively).

So far we have successfully obtained blue, green, and violet emissions from the same TTC4L molecule. However, the colors available in the TTC4L solution are not limited to these. We noticed that at medium DEAB concentrations such as 12 mM, the emission peak is rather broad, and actually extends beyond 600 nm. Therefore, it is possible to generate more narrow colors simply by varying the excitation wavelength. Curves 4 and 5 in Fig. 3a demonstrate that the emissions keep red-shifting upon increasing the excitation wavelength. We may even obtain yellow and orange emissions when exciting the same solution at 520 nm. Inset image 5 in Fig. 3 demonstrates the yellow-orange Tyndall light pass obtained by excitation of the solution with a 532 nm green laser. The actual color of the light pass is orange which looks like yellow in the photo. The location of this orange color was demonstrated in the CIE plot (Fig. 3b) with coordinates of (0.507, 0.491). It can be clearly visualized in the CEI plot that the colors obtained in the TTC4L system may cover most of the visible light region except red and deep purple.

As already discussed, the emission spectra is rather broad in the wide DEAB concentration range of 5–20 mM, which allows continual tuning of the emissions from violet to orange by simply increasing the concentration of DEAB gradually.

### Molecular mechanism of the multiple color emissions

In order to gain more insight into the emission, time-correlated single-photon-counting measurements<sup>45</sup> were carried out for the TTC4L systems with and without DEAB to provide information about the molecular states of TTC4L. Two lifetimes were obtained from the fluorescence decay curves for the TTC4L aqueous suspensions without DEAB, suggesting the presence of two states of TTC4L. The shorter one around 0.3 ns can be ascribed to the non-aggregated single TTC4L molecules (monomers) owing to a fast intersystem crossing to the triplet state, whereas the longer one around 2.7 ns (ESI, Table S1†) originates from the H-aggregated TTC4L molecules.<sup>47–50</sup> The time-correlated single-photon-counting measurements also suggest that the amounts of TTC4L in the monomeric state and in aggregates are about 15 and 85%, respectively, (Fig. 4a) regardless of the concentrations. This means that in the self-assembled systems, the emission from the monomers is predominantly overwhelmed by that of TTC4L in the aggregate states.

The situation will be different when the cationic surfactant DEAB is added to the system. The percentage of monomers increases with increasing DEAB concentration (Fig. 4b), which amounts to nearly 95% at 30 mM DEAB. Meanwhile, the percentage of aggregated TTC4L keeps decreasing and become negligible at 30 mM DEAB. The most remarkable phenomenon is the occurrence of excimers with a lifetime longer than 5 ns at medium DEAB concentrations.<sup>26</sup> There is approximately 19% of TTC4L in the form of excimers at 12 mM DEAB. Although this percentage is not dominant in the system, the emission is so overwhelming that the system gives a characteristic green emission.

The change of the molecular state of TTC4L upon addition of DEAB was also reflected in the UV spectra. In Fig. 5 we show the change of the UV spectra of TTC4L with increasing DEAB concentration. Without DEAB, 0.1 mM TTC4L gives a broad

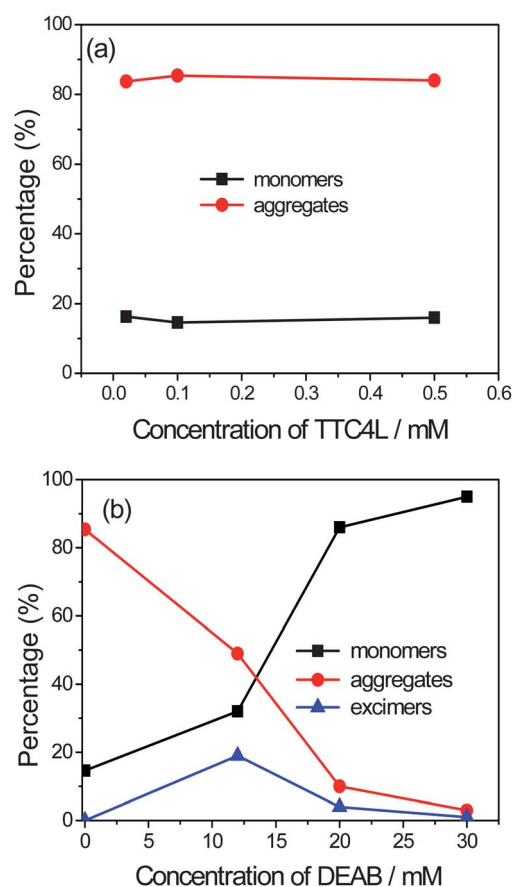


**Fig. 4** (a) Percentage of TTC4L molecules in different states determined from fluorescence lifetime measurements. (b) Variation of the percentage of different fluorescent species in the TTC4L solutions with increasing DEAB concentration.

absorption centered at 343 nm, which is caused by the  $\pi$ - $\pi^*$  electron transition of terthiophene groups<sup>31</sup> in the aggregated states. Upon the addition of DEAB to this solution, the intensity of this absorption increases significantly and the position shifts toward red. It can be seen from Fig. 5 that in the presence of 12 mM DEAB, the peak is further broadened and an additional

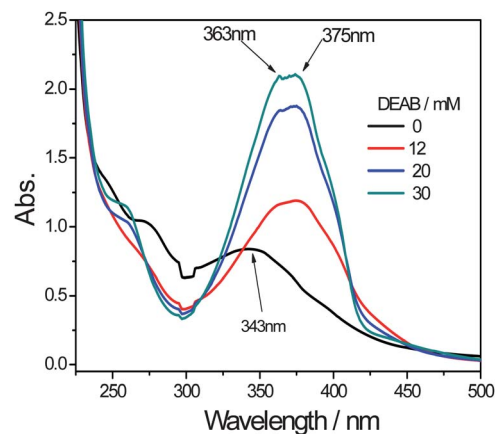


**Fig. 5** UV spectra of 0.1 mM TTC4L in the presence of DEAB at various concentrations.



peak at around 360 nm is roughly identified.<sup>29</sup> This suggests that at this stage, TTC4L in the monomeric state is present. It is also very clear that the UV spectra exhibit a featureless shoulder peak at around 390–400 nm, indicating the presence of excimers.<sup>26</sup> At much higher DEAB concentrations, such as 20 and 30 mM, the intensity for the monomeric TTC4L absorption is further enhanced, whereas the shoulder become less impressive. These features are in perfect agreement with the results obtained from the fluorescence lifetime measurements in Fig. 4b, which unambiguously confirmed the change of molecular states of TTC4L with addition of DEAB at different concentrations. However, both the fluorescence and the UV measurements suggest that in the wide range of medium DEAB concentrations, it is difficult to get narrowly distributed  $\pi$ – $\pi$  distances. We may obtain a narrowly distributed  $\pi$ – $\pi$  distance larger than 7 Å at very high DEAB concentrations, for example, over 20 mM in this case. Otherwise, the addition of a small amount of DEAB always triggered polydisperse  $\pi$ – $\pi$  distances. However, such multiple possibilities of the  $\pi$ – $\pi$  distance are not undesired in this system, because it is this polydispersed  $\pi$ – $\pi$  distance that allows the continuous generation of multicolor fluorescence.

The change of molecular states of TTC4L with increasing surfactants is also a reflection of the evolution of the self-assembled structures in the system. To verify this, dynamic light scattering measurements were carried out. As demonstrated in Fig. 6, the size of the particles in the 0.5 mM TTC4L system is progressively decreased with increasing DEAB concentration. Without addition of DEAB, the TTC4L self-assemble into particles with an average hydrodynamic radius of around 100 nm, which have been previously verified to be vesicles (Fig. 1b). In contrast, upon addition of 2 mM DEAB, another group of particles with an average hydrodynamic radius of around 4 nm were found to come into co-existence with the vesicles. At 4 mM DEAB, the scattering from the smaller particles becomes dominant, which is at the cost of the lowering of the scattering from the larger ones. If we consider that the scattering intensity is proportional to the particle radius with the order of  $10^4$ , it can be estimated that in the presence of 2–4 mM DEAB, the number of large vesicles in the 0.5 mM TTC4L system is almost negligible compared with the quantity of the small particles. Considering the fact that the extending length of the

TTC4L molecule is about 2.2 nm, these smaller particles are probably micellar clusters co-assembled from TTC4L and DEAB. This suggests that the addition of DEAB into the TTC4L suspension has transformed the self-assembly of TTC4L into a co-assembly of TTC4L and DEAB, thus the intermolecular distance between the terthiophene groups is effectively increased. We can exclude the possibility that the smaller particles might be the micelles of DEAB itself as the extending length of DEAB is about 1.5 nm, so that the radius of DEAB micelles should not exceed this value. This was indeed the case. As demonstrated in Fig. 6, at a concentration far beyond the critical micellar concentration (CMC), the average hydrodynamic radius of DEAB micelles is roughly 1 nm. Thus, the control experiments have clearly verified that the smaller particles in the TTC4L–DEAB mixed solutions are indeed the co-assembly from these two components. However, the fluorescence lifetime measurements (Fig. 4b) suggest that there are still self-aggregated domains of TTC4L in the small aggregates, but the size of the aggregated domains are considerably decreased which is inferred from the shorter fluorescence lifetimes (1.3 ns, Table S2†).<sup>48</sup> According to Fig. 4b, the fraction of TTC4L in these domains is about 49%. We believe that such ‘aggregated TTC4L’ is probably a result of irregular overlap of the terthiophene groups in the micellar core, which leads to 4–7 Å separations between the terthiophene groups. This allows for the formation of excimers, and a green emission occurs. At a DEAB concentration greater than 20 mM, each micellar cluster may contain only one TTC4L molecule so that only a monomeric emission is observed. The whole process of aggregate transition is illustrated in Scheme 2.

### Generality of the surfactant-assisted multicolor emissions

Surfactant-induced multicolor emissions from TTC4L molecules can be generalized to a large variety of surfactants. Non-ionic surfactant such as TX-100, zwitterionic ones like TPPS and C<sub>14</sub>DMAO, as well as other cationic surfactants, such as CTAB, and even gemini-type cationic surfactants, may have a similar effect as DEAB (Fig. S3–S6†). In contrast, negatively charged surfactants such as SDS, which carries the same charge as TTC4L, are less effective at breaking the self-assembly of TTC4L into a mixed co-assembly (Fig. S7†). Therefore, the electrostatic interactions should play a key role in the present strategy, which

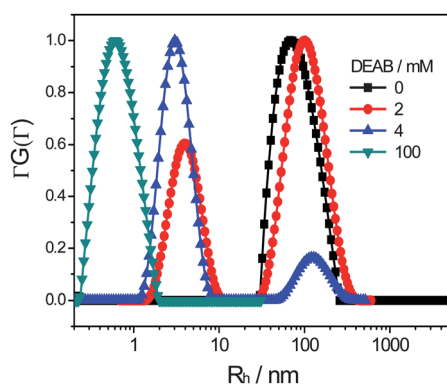
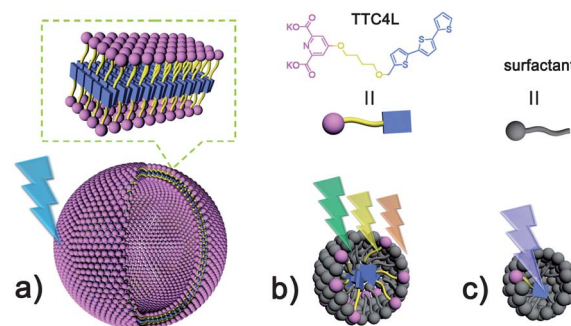


**Fig. 6** DLS results of 0.5 mM TTC4L in the presence of different concentrations of DEAB. The curve with 100 mM DEAB is the result from the DEAB aqueous solution where no TTC4L is present.



**Scheme 2** Illustration of the arrangement of TTC4L molecules under various conditions. (a) represents the self-assembly formed by TTC4L, whereas (b) and (c) are the co-assemblies between TTC4L and surfactants with increasing surfactant concentration.

may provide a higher efficiency in triggering the desired emissions. Actually, the stronger the interaction between TTC4L and surfactants, the less surfactant is required to reach the same emissions. It was found that if DEAB was replaced by cationic surfactants with lower CMCs, such as CTAB and  $C_{12}C_4C_{12}(Et)$ ,<sup>51</sup> the critical surfactant concentration desired for triggering fluorescence transition was much lower. For instance, 0.5 mM CTAB or  $C_{12}C_4C_{12}(Et)$  is enough to alter the fluorescence of TTC4L from blue to green, as demonstrated in Fig. 7a.

The effect of the surfactant on the multicolor emission was also compared with that obtained by host–guest chemistry. Two types of pristine cyclodextrins ( $\beta$ - and  $\gamma$ -CDs) were used to form complexes with a terthiophene moiety.<sup>26,52,53</sup> Although  $^1H$  NMR measurements confirmed the successful inclusion of TTC4L into the cavity of  $\beta$ -CD (Fig. S8†), this only affects the intensity of the emission, which doesn't produce a considerable effect on the fluorescence emission (Fig. S9†).<sup>52</sup> In analogy, if  $\gamma$ -CD is used, an obvious red-shift of the emission yet negligible blue-shift can be triggered, as demonstrated in Fig. 7b. The occurrence of the green component is attributed to the inclusion of two TTC4L molecules in the larger cavity of  $\gamma$ -CD,<sup>54</sup> which is beneficial to the formation of excimers.<sup>26</sup> However, it seems that the fraction of excimers generated in this host–guest chemistry is rather low so that only a transition color between blue and green was obtained.

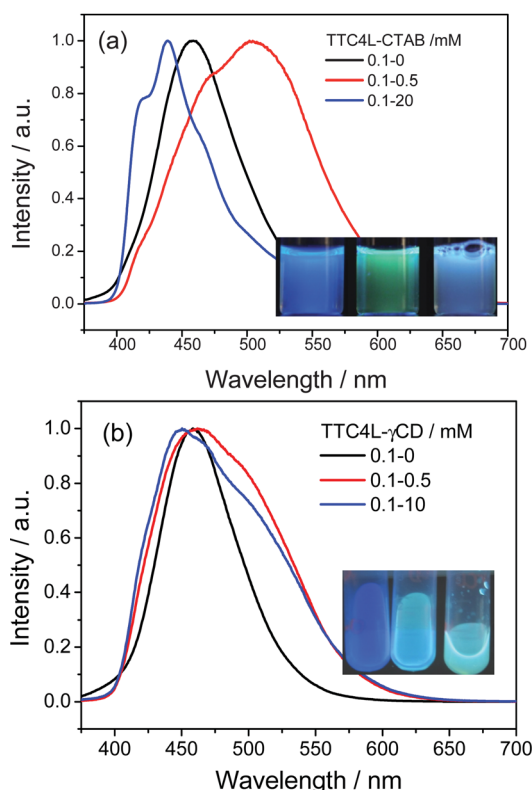


**Fig. 7** (a) Normalized emission spectra of 0.1 mM TTC4L in the presence of CTAB of various concentrations (excited at 360 nm). The inset shows the corresponding colors for 0.1 mM TTC4L with 0, 0.5 and 20 mM CTAB under 365 nm UV light. (b) Normalized emission spectra of 0.1 mM TTC4L in the presence of  $\gamma$ -CD of various concentrations (excited at 360 nm). The inset shows the corresponding colors for 0.1 mM TTC4L with 0, 0.5 and 10 mM  $\gamma$ -CD under 365 nm UV light.

Therefore, the surfactant-assisted strategy shows a clear superiority to host–guest chemistry.

## Conclusions

In summary, we have provided a surfactant-assisted unimolecular strategy to generate multicolor fluorescent emissions from the same fluorescent terthiophene-amphiphile TTC4L. Upon tuning the intermolecular distance between the terthiophene groups by changing the self-assembly of TTC4L to co-assembly with various surfactants, we may obtain emissions from violet to orange which cover most of the visible light region without changing and modifying the structure of the TTC4L. It is a general approach which is applicable to many surfactants and fluorescent molecules with similar properties. We believe that it is far beyond an interesting example of ‘multicolor emissions from one molecular platform’, but also an innovative employment of molecular assemblies in fabricating advanced laminating materials.

## Acknowledgements

This research was supported by the National Natural Science Foundation of China (20903005, 21173011, 51121091, 21073006), and the Doctorial Fund of Ministry of Education of China. We would like to thank Prof. Zichen Li for his advice on the synthesis.

## References

- G. J. He, D. Guo, C. He, X. L. Zhang, X. W. Zhao and C. Y. Duan, *Angew. Chem., Int. Ed.*, 2009, **48**, 6132–6135.
- H. Yu, D. Liao, M. B. Johnston and B. Li, *ACS Nano*, 2011, **5**, 2020–2025.
- K. Tanabe, Y. Suzui, M. Hasegawa and T. Kato, *J. Am. Chem. Soc.*, 2012, **134**, 5652–5661.
- V. Bedekar, D. P. Dutta, M. Mohapatra, S. V. Godbole, R. Ghildiyal and A. K. Tyagi, *Nanotechnology*, 2009, **20**, 125707.
- B.-K. An, S. H. Gihm, J. W. Chung, C. R. Park, S.-K. Kwon and S. Y. Park, *J. Am. Chem. Soc.*, 2009, **131**, 3950–3957.
- S. Saito, K. Nakakura and S. Yamaguchi, *Angew. Chem., Int. Ed.*, 2012, **51**, 714–717.
- M. Zambianchi, F. Di Maria, A. Cazzato, G. Gigli, M. Piacenza, F. D. Sala and G. Barbarella, *J. Am. Chem. Soc.*, 2009, **131**, 10892–10900.
- H. S. Joshi, R. Jamshidi and Y. Tor, *Angew. Chem., Int. Ed.*, 1999, **38**, 2722–2725.
- E. Kim, M. Koh, B. J. Lim and S. B. Park, *J. Am. Chem. Soc.*, 2011, **133**, 6642–6649.
- E. Kim, M. Koh, J. Ryu and S. B. Park, *J. Am. Chem. Soc.*, 2008, **130**, 12206.
- Z. Zhao, C. Deng, S. Chen, J. W. Y. Lam, W. Qin, P. Lu, Z. Wang, H. S. Kwok, Y. Ma, H. Qiu and B. Z. Tang, *Chem. Commun.*, 2011, **47**, 8847–8849.
- L. Jiang, Y. Yan, M. Drechsler and J. Huang, *Chem. Commun.*, 2012, **48**, 7347–7349.
- M. Freitag, L. Gundlach, P. Piotrowiak and E. Galoppini, *J. Am. Chem. Soc.*, 2012, **134**, 3358–3366.
- N. Barooah, J. Mohanty, H. Pal and A. C. Bhasikuttan, *Phys. Chem. Chem. Phys.*, 2011, **13**, 13117–13126.
- A. K. Mandal, M. Suresh, P. Das and A. Das, *Chem.–Eur. J.*, 2012, **18**, 3906–3917.
- M. Suresh, A. K. Mandal, M. K. Kesharwani, N. N. Adarsh, B. Ganguly, R. K. Kanaparthi, A. Samanta and A. Das, *J. Org. Chem.*, 2011, **76**, 138–144.
- C. Li, J. Li and X. Jia, *Org. Biomol. Chem.*, 2009, **7**, 2699–2703.
- A. C. Bhasikuttan, H. Pal and J. Mohanty, *Chem. Commun.*, 2011, **47**, 9959–9971.

- 19 G. Pistolis, *Chem. Phys. Lett.*, 1999, **304**, 371–377.
- 20 S. Sau, B. Solanki, R. Orpreco, J. Van Stam and C. H. Evans, *J. Inclusion Phenom. Macrocyclic Chem.*, 2004, **48**, 173–180.
- 21 D. A. Stone, A. S. Tayi, J. E. Goldberger, L. C. Palmer and S. I. Stupp, *Chem. Commun.*, 2011, **47**, 5702–5704.
- 22 M. Jenart, C. Niebel, J. Y. Balandier, J. Leroy, A. Mignolet, S. Stas, A. Van Vooren, J. Cornil and Y. H. Geerts, *Tetrahedron*, 2012, **68**, 349–355.
- 23 G. Barbarella, L. Favaretto, G. Sotgiu, M. Zambianchi, A. Bongini, C. Arbizzani, M. Mastragostino, M. Anni, G. Gigli and R. Cingolani, *J. Am. Chem. Soc.*, 2000, **122**, 11971–11978.
- 24 I. F. Perepichka, D. F. Perepichka, H. Meng and F. Wudl, *Adv. Mater.*, 2005, **17**, 2281–2305.
- 25 A. Mishra, C. Q. Ma and P. Bauerle, *Chem. Rev.*, 2009, **109**, 1141–1276.
- 26 S. De Feyter, J. van Stam, F. Imans, L. Viaene, F. C. De Schryver and C. H. Evans, *Chem. Phys. Lett.*, 1997, **277**, 44–50.
- 27 W. W. Tsai, L. S. Li, H. G. Cui, H. Z. Jiang and S. I. Stupp, *Tetrahedron*, 2008, **64**, 8504–8514.
- 28 M. Fujitsuka, D. W. Cho, J. Ohshita, A. Kunai and T. Majima, *J. Phys. Chem. C*, 2007, **111**, 1993–1998.
- 29 V. Percec, M. Glodde, T. K. Bera, Y. Miura, I. Shivanovskaya, K. D. Singer, V. S. K. Balagurusamy, P. A. Heiney, I. Schnell, A. Rapp, H. W. Spiess, S. D. Hudson and H. Duan, *Nature*, 2002, **417**, 384–387.
- 30 W. Mroz, J. P. Bombenger, C. Botta, A. O. Biroli, M. Pizzotti, F. De Angelis, L. Belpassi, R. Tubino and F. Meinardi, *Chem.–Eur. J.*, 2009, **15**, 12791–12798.
- 31 V. D. Deepak and P. R. Sundararajan, *J. Phys. Chem. B*, 2011, **115**, 8458–8464.
- 32 D. A. Stone, L. Hsu and S. I. Stupp, *Soft Matter*, 2009, **5**, 1990–1993.
- 33 A. A. Sobczuk, S. Tamaru and S. Shinkai, *Chem. Commun.*, 2011, **47**, 3093–3095.
- 34 L. Zalewski, S. Brovelli, M. Bonini, J. M. Mativetsky, M. Wykes, E. Orgiu, T. Breiner, M. Kastler, F. Dotz, F. Meinardi, H. L. Anderson, D. Beljonne, F. Cacialli and P. Samori, *Adv. Funct. Mater.*, 2011, **21**, 834–844.
- 35 T. Lu, F. Han, G. Mao, G. Lin, J. Huang, X. Huang, Y. Wang and H. Fu, *Langmuir*, 2007, **23**, 2932–2936.
- 36 D. G. Whitten, *Acc. Chem. Res.*, 1993, **26**, 502–509.
- 37 S. Selector, O. Fedorova, E. Lukovskaya, A. Anisimov, Y. Fedorov, N. Tarasova, O. Raitman, F. Fages and V. Arslanov, *J. Phys. Chem. B*, 2012, **116**, 1482–1490.
- 38 N. C. Maiti, S. Mazumdar and N. Periasamy, *J. Phys. Chem. B*, 1998, **102**, 1528–1538.
- 39 T. Hasobe, S. Fukuzumi and P. V. Kamat, *J. Am. Chem. Soc.*, 2005, **127**, 11884–11885.
- 40 S. Ghosh, X.-Q. Li, V. Stepanenko and F. Würthner, *Chem.–Eur. J.*, 2008, **14**, 11343–11357.
- 41 C. Strassler, N. E. Davis and E. T. Kool, *Helv. Chim. Acta*, 1999, **82**, 2160–2171.
- 42 Y. Yan, W. Xiong, J. B. Huang, Z. C. Li, X. S. Li, N. N. Li and H. L. Fu, *J. Phys. Chem. B*, 2005, **109**, 357–364.
- 43 T. Lu, Z. Li, J. Huang and H. Fu, *Langmuir*, 2008, **24**, 10723–10728.
- 44 H. Kashida, H. Asanuma and M. Komiyama, *Chem. Commun.*, 2006, 2768–2770.
- 45 M. R. Molla and S. Ghosh, *Chem.–Eur. J.*, 2012, **18**, 1290–1294.
- 46 M. Kumar and S. J. George, *Nanoscale*, 2011, **3**, 2130–2133.
- 47 T. M. Clarke, K. C. Gordon, W. M. Kwok, D. L. Phillips and D. L. Officer, *J. Phys. Chem. A*, 2006, **110**, 7696–7702.
- 48 D. Anastopoulos, M. Fakis, G. Mousdis, V. Giannetas and P. Persephonis, *Synth. Met.*, 2007, **157**, 30–34.
- 49 M. Belletete, L. Mazerolle, N. Desrosiers, M. Leclerc and G. Durocher, *Macromolecules*, 1995, **28**, 8587–8597.
- 50 P. Hrdlovic, J. Krajcovic and D. Vegh, *J. Photochem. Photobiol., A*, 2001, **144**, 73–81.
- 51 T. Lu, Y. R. Lan, C. J. Liu, J. B. Huang and Y. L. Wang, *J. Colloid Interface Sci.*, 2012, **377**, 222–230.
- 52 C. H. Evans, S. DeFeyter, L. Viaene, J. vanStam and F. C. DeSchryver, *J. Phys. Chem.*, 1996, **100**, 2129.
- 53 B. Gombojav, N. Namsrai, T. Yoshinari, S. I. Nagasaka, H. Itoh and K. Koyama, *J. Solid State Chem.*, 2004, **177**, 2827.
- 54 Y. Yan, L. Jiang and J. Huang, *Phys. Chem. Chem. Phys.*, 2011, **13**, 9074.